

---

# Promotional effect of iron on the activity of TiO<sub>2</sub> in the production of adipic acid

Ameur Nawal<sup>1,2,\*</sup>, Bachir Redouane<sup>2</sup>, Bedrane Sumeya<sup>2</sup>,  
Choukchou-Braham Abderrahim<sup>2</sup>

1. High School of Electrical and Energetic Engineering of Oran (ESGEE), Algeria

2. Laboratory of Catalysis and Synthesis in Organic Chemistry (LCSCO),  
Tlemcen, Algeria

ameurnawel@yahoo.fr

---

**ABSTRACT.** Designing a new process for the synthesis of adipic acid using green conditions is important to achieve its sustainable development. In this paper, we present a synthesis of adipic acid in one step under a green and mild reaction conditions. The oxidation of cyclohexene to adipic acid using molecular oxygen as oxidant was carried out over different heterogeneous X%Fe<sub>2</sub>O<sub>3</sub>/TiO<sub>2</sub> catalysts. The catalysts exhibited good conversion (32.5%) and high product (Adipic Acid) selectivity (91.4%). The catalysts were characterized by ICP AES analysis, N<sub>2</sub> adsorption–desorption Isotherm (BET), FT-IR, DR/UV-Vis and DRX techniques. A comparison between the effect of the preparation method; impregnation in this work and sol gel method in previous work of the catalyst is discussed.

**RÉSUMÉ.** Choisir un nouveau processus pour la synthèse de l'acide adipique en employant des conditions qui respectent la chimie verte est important pour un développement convenable. Dans cet article, nous présentons la synthèse de l'acide adipique en une seule étape dans des conditions douces et qui obéit aux critères de la chimie verte. L'oxydation du cyclohexène en acide adipique en utilisant l'oxygène moléculaire comme oxydant a été réalisée sur différents catalyseurs hétérogènes X%Fe<sub>2</sub>O<sub>3</sub>/TiO<sub>2</sub>. Les catalyseurs ont montré une bonne conversion (32.5%) et une sélectivité importante vers la production de l'acide adipique (91.4%). Les catalyseurs ont été caractérisés par analyse ICP, BET, FT-IR, UV-Vis en RD and DRX. Une comparaison entre l'effet de la méthode de préparation; l'imprégnation dans ce travail et la méthode sol gel dans un travail précédent, est également discutée

**KEYWORDS:** oxidation, cyclohexene, adipic acid, iron, titania.

**MOTS-CLÉS:** oxydation, cyclohexène, acide adipique, Fer, titane.

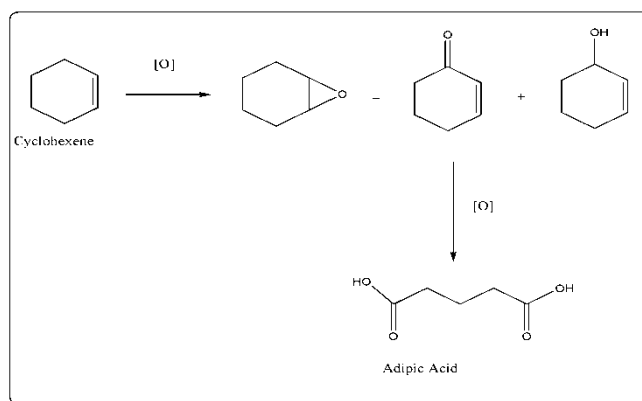
---

DOI:10.3166/ACSM.41.173-188 © 2017 Lavoisier

## 1. Introduction

Adipic acid is an important bulk chemical product in different industrial chemistry process. It is largely used in the manufacture of polyurethanes, plasticizers and particularly nylon 6,6 polyamide (Castellan *et al.*, 1991). In fact the global adipic acid capacity increases steadily. It is expected to reach 3.3 million tons per year in 2016 when it was about 2.6 million tons per year in 2010.

Actually, it is produced from cyclohexane in two steps. The first step is the production of a mix of cyclohexanone and cyclohexanol by an oxidation of cyclohexane using cobalt salts as catalysts. The mix of cyclohexanone and cyclohexanol is oxidized then after by nitric acid to adipic acid in the second step. This process is cost-effective and has a great defect that is a low conversion of cyclohexane in the first step. In addition, it is a pollutant process, because it releases an important amount of nitrous oxide as a stoichiometric waste product due to the utilization of nitric acid.  $N_2O$  is known to cause some environmental problems such as the greenhouse effect and ozone depletion.



*Scheme 1. Production of adipic acid from oxidation of cyclohexene*

The oxidation of cyclohexene is a good alternative to produce adipic acid in one pot with an environmentally friendly process (Bart and Cavallaro, 2015). Cyclohexene oxidation is an important industrial reaction. This reaction lead to the formation in a premiere oxidation of different important products such as: cyclohexene oxide, cyclohex-1,2-enone and cyclohex-1,2-enol (scheme 1). These products are used as bulk chemicals for the synthesis of different drugs, pesticides, cosmetics products (Schwidder *et al.*, 2005, Sreethawong *et al.*, 2006, Dapurkar *et al.*, 2008, Li *et al.*, 2009, Jiang *et al.*, 2010, Van de Vyver and Román-Leshkov, 2013).

Different oxidants are used in cyclohexene oxidation such as:  $H_2O_2$  (Schwidder *et al.*, 2005, Sreethawong *et al.*, 2006), TBHP (Li *et al.*, 2009, Ameer *et al.*, 2014, Ameer *et al.*, 2013) and molecular oxygen (Cai *et al.*, 2010). In some cases an over

oxidation of the premiere oxidation products is observed, allowing to obtain high added value molecules. Indeed, Heiko Weiner and coll. (Weiner *et al.*, 2003) reported that nearly 70 products can be obtained by an over oxidation of cyclohexene. Among these products adipic acid is the most important.

Sato and his group (Sato *et al.*, 1998) were the first to produce the adipic acid directly by oxidation of cyclohexene. They used a tungsten-based homogeneous catalyst and a quaternary ammonium salts as phase transfer catalysts. After that, different catalytic systems were proposed (Van de Vyver and Román-Leshkov, 2013, Reed and Hutchison, 2000, Jähnisch *et al.*, 2004, Cheng *et al.*, 2007, Bohström *et al.*, 2010, Jin *et al.*, 2011, Wen *et al.*, 2012, Vafaezadeh *et al.*, 2012, Behera *et al.*, 2013, Ghosh *et al.*, 2014). Nevertheless, these systems have some defaults, such as lower product yields, requirement of acidic media, a polluting process (Jin *et al.*, 2011, Lapisardi *et al.*, 2005, Wang *et al.*, 2013, Vafaezadeh and Hashemi, 2014, Ameer *et al.*, 2014, Ameer *et al.*, 2013, Meng *et al.*, 2015).

In previous work of our group we presented a green route to produce adipic acid by direct oxidation of cyclohexene by using molecular oxygen as oxidant on x%Fe<sub>2</sub>O<sub>3</sub>-TiO<sub>2</sub> materials (prepared by sol gel method). An excellent selectivity was achieved; about 97%; and was influenced by iron loading. All in all, we conclude that this way is very important to produce adipic acid from cyclohexene. So, this paper is a continuation of our previous work; still the study of the catalytic activity of Fe<sub>2</sub>O<sub>3</sub> doped TiO<sub>2</sub> (P25, commercial) materials prepared by conventional impregnation and employed on the cyclohexene oxidation by O<sub>2</sub>.

## 2. Results and discussions

Different Fe<sub>2</sub>O<sub>3</sub>/TiO<sub>2</sub> catalysts were prepared by varying the Ti/Fe molecular ratio. These materials and their acronyms are reported in Table 1.

Table 1. Different materials and their acronyms

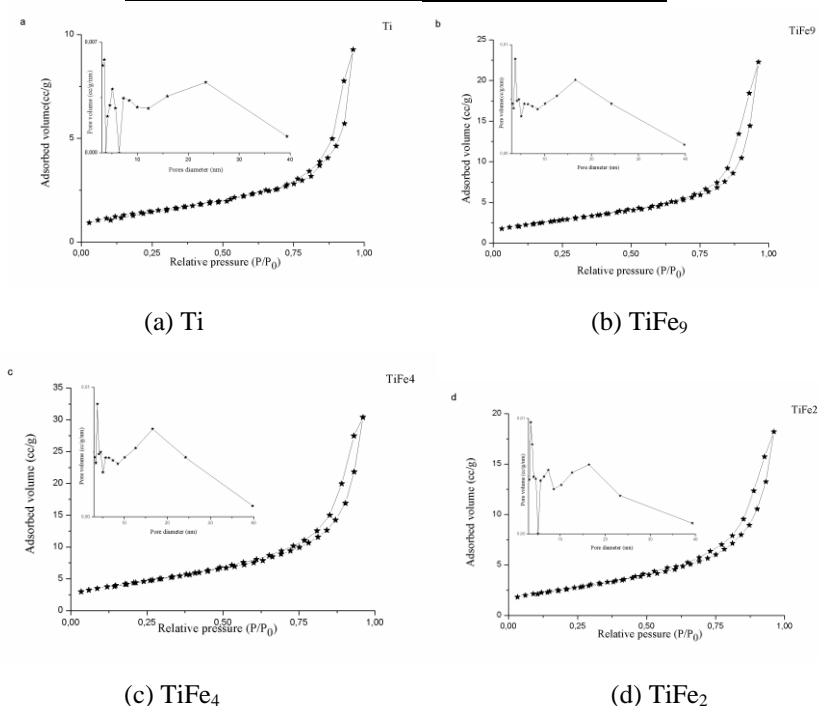
	TiO <sub>2</sub>	Fe <sub>2</sub> O <sub>3</sub> /TiO <sub>2</sub>		
Ti/Fe	-----	2	4	9
Acronym	Ti	TiFe <sub>2</sub>	TiFe <sub>4</sub>	TiFe <sub>9</sub>

The results of ICP-AES analysis of the different materials indicate that the iron was effectively impregnated on TiO<sub>2</sub> (Table 2). The Fe<sub>2</sub>O<sub>3</sub> content ranges from 6.4% and 9.8%.

Nitrogen adsorption-desorption revealed a type IV adsorption isotherm corresponding to a mesoporous structure according to the IUPAC and a type H3 loop hysteresis ( $0.7 < P/P_0 < 0.9$ ) in all cases (Figure 1).

Table 2. ICP-AES analysis of iron

Materials	Moles of Fe/g of oxides*10-5	%Fe <sub>2</sub> O <sub>3</sub>
TiFe <sub>9</sub>	40.3	6.4
TiFe <sub>4</sub>	51.6	8.2
TiFe <sub>2</sub>	61.6	9.8

Figure 1. N<sub>2</sub> adsorption-desorption isotherm

The corresponding textural parameters are also reported in Table 3. The pore size distribution is heterogeneous for all materials. Otherwise, the introduction of iron induces a little increase in the BET surface area and porous volume of TiO<sub>2</sub>. This is probably due to the increase of its lattice further to the insertion of iron. We noticed that the preparation of the same materials by sol gel method lead to the best area.

The XRD patterns of all materials are reported in Figure 2. All the peaks (Figure 2a) match well with the typical spectrum of the commercial TiO<sub>2</sub> (P25). Indeed, the peaks revealed TiO<sub>2</sub> crystalline regions anatase and rutile forms (Table 4). The TiFe materials spectra (Figure 2b, 2c, 2d) revealed three peaks at  $2\theta = 22^\circ$  attributed to the maghemite-C phase of Fe<sub>2</sub>O<sub>3</sub> and at  $2\theta = 24.2^\circ$  and  $35.4^\circ$  attributed to the hematite phase of Fe<sub>2</sub>O<sub>3</sub>. Moreover, all TiFe materials spectra show the

characteristic peaks of TiO<sub>2</sub> with a little shift (Figure 3). For example, the peak situated at  $2\theta = 25.28^\circ$  is shifted to  $2\theta = 25.17^\circ$ . This indicates an expansion of TiO<sub>2</sub> lattice that can be explained by the insertion of iron atoms in the TiO<sub>2</sub> lattices. In addition, the iron and titanium atoms have a similar atomic radius: 0.64 and 0.68 Å respectively.

Table 3. BET textural parameters of Ti and TiFe materials

Materials	SBET (m <sup>2</sup> .g <sup>-1</sup> )	SBJHD(m <sup>2</sup> .g <sup>-1</sup> )	Porous volume (cc/g)	Pore diameters (nm)
Ti	41	33	0.11	3.5
TiFe9	51	48	0.14	3.6
TiFe4	52	47	0.15	3.7
TiFe2	45	45	0.13	3.4

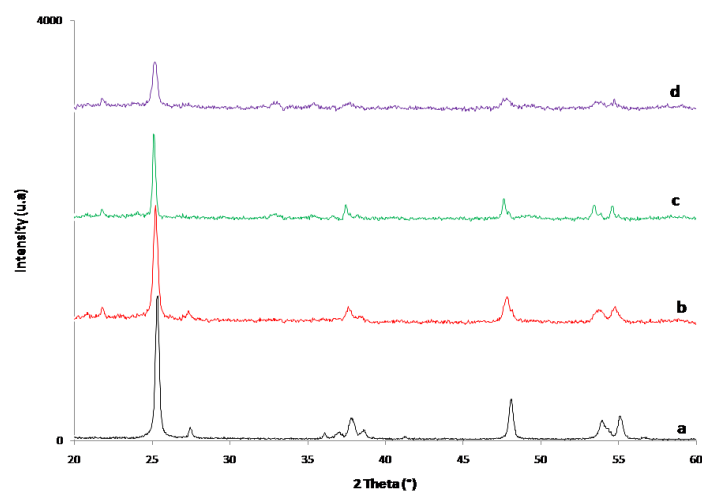


Figure 2. The XRD spectra of: (a) Ti, (b) TiFe<sub>9</sub>, (c) TiFe<sub>4</sub>, and (d) TiFe<sub>2</sub>

The materials were characterized by diffuse reflectance UV-vis spectroscopy (DR/UV-vis) in order to study the coordination environment of Ti and Fe. Figure 4 shows a comparison between the spectra of TiO<sub>2</sub> and the different TiFe materials. We can see for TiO<sub>2</sub> (Figure 4a) an absorption only in the UV part (200–400 nm). However, the TiFe materials have bands in both the UV and the visible parts of the spectra.

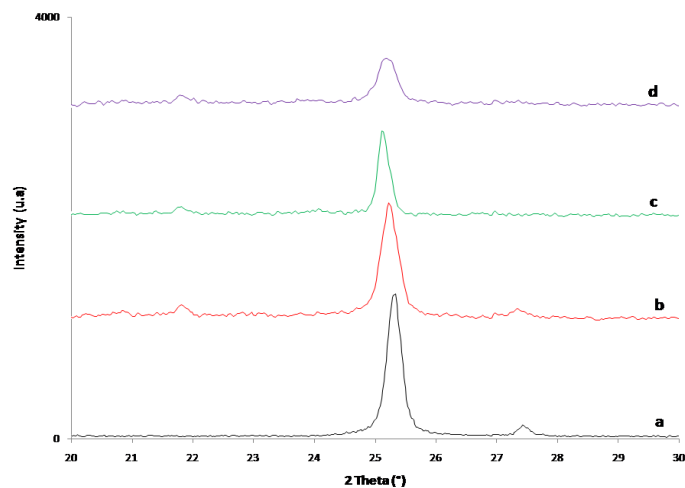


Figure 3. A zoom ( $2\theta = 20^\circ\text{-}30^\circ$ ) on the XRD spectra of: (a) Ti, (b)  $\text{TiFe}_9$ , (c)  $\text{TiFe}_4$ , and (d)  $\text{TiFe}_2$

Table 4. XRD peaks of  $\text{TiO}_2$

$2\theta$	Plan	Phase
$25.28^\circ$	(101)	Anatase
$37.01^\circ$	(103)	
$37.76^\circ$	(004)	
$38.58^\circ$	(112)	
$48.06^\circ$	(200)	
$53.90^\circ$	(105)	
$55.06^\circ$	(211)	Rutile
$27.40^\circ$	(110)	
$37.07^\circ$	(101)	
$41.25^\circ$	(111)	

The deconvolution of the  $\text{TiO}_2$  spectrum (Figure 5a) shows three bands located at 207, 256 and 347 nm. They are characteristic of anatase phase and are assigned to the  $\text{Ti}^{4+} \rightarrow \text{OH}$ ,  $\text{O}^-$  (Cozzolino *et al.*, 2007) charge transfer band for the  $\text{Ti}^{4+}$  cations

in a tetrahedral environment (Nur, 2006). We see also a band at 302 nm. It is assigned to the rutile phase.

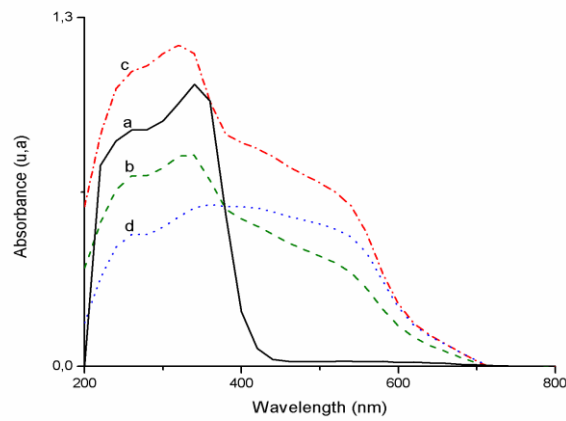


Figure 4. DR/UV-Vis characterization of: (a) Ti, (b) TiFe<sub>9</sub>, (c) TiFe<sub>4</sub>, and (d) TiFe<sub>2</sub>

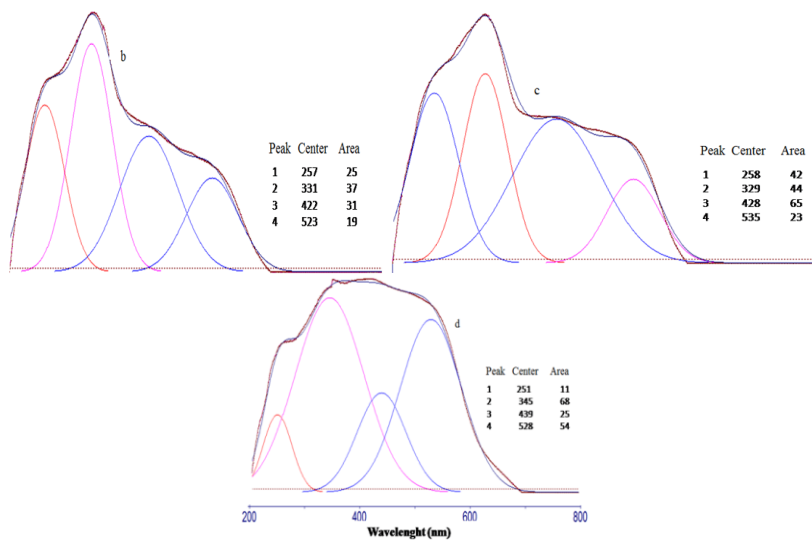


Figure 5. DRUV-Vis spectra deconvoluted bands of: (a) Ti, (b) TiFe<sub>9</sub>, (c) TiFe<sub>4</sub>, and (d) TiFe<sub>2</sub>

For TiFe materials, the deconvolution of the spectra (Figures 5b, 5c, 5d) indicates that the anatase phase characteristic bands (257 nm and 347 nm) are still available. Whereas, the band assigned to rutile phase doesn't exist. Moreover, we observed two new bands located at 422 nm and 523 nm for TiFe<sub>9</sub>. They are assigned to  $\alpha$ -Fe<sub>2</sub>O<sub>3</sub> particles. Indeed, the first band is related to d-d transition of  $\alpha$ -Fe<sub>2</sub>O<sub>3</sub> particles and the second one is attributed to the 6A<sub>1g</sub>→4T<sub>1g</sub> and 6A<sub>1g</sub>→4T<sub>2g</sub> transitions in  $\alpha$ -Fe<sub>2</sub>O<sub>3</sub> oxides (Schwidder *et al.*, 2005, Prieto-Centurion *et al.*, 2012). We note a little shift of these bands when the amount of iron is rising. This is probably due to the change of Fe<sub>2</sub>O<sub>3</sub> particle sizes (Schwidder *et al.*, 2005).

The FTIR spectrum of TiO<sub>2</sub> (Figure 6 a) shows an intense absorption band situated between 400 and 900 cm<sup>-1</sup> and centered at 630 cm<sup>-1</sup>. This band is attributed to the vibration of Ti-O bond of the anatase phase of TiO<sub>2</sub> (Ahmed *et al.*, 2013).

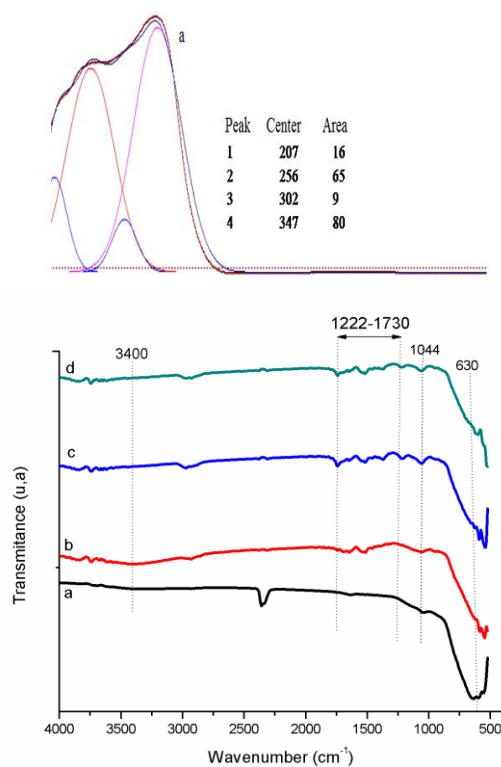


Figure 6. Infrared spectra of (a) Ti, (b) TiFe<sub>9</sub>, (c) TiFe<sub>4</sub>, and (d) TiFe<sub>2</sub>

We noticed that the intensity of this absorption decreased by adding iron (Figure 6b, 6c, 6d) to TiO<sub>2</sub>. Otherwise, we observed a new band at 1044 cm<sup>-1</sup> in the FTIR spectra of TiFe comparing to TiO<sub>2</sub>. This band is related to the vibration of the

heterogeneous Ti-O-Fe bond. These results indicate an interaction between Ti and iron and confirmed the insertion of iron in the TiO<sub>2</sub> lattice.

Figure 7 shows micrographs of doped-TiO<sub>2</sub> materials. The micrographs indicate a spherical shape with different size of the particles of the materials under study and confirm good crystallization of the materials. However, the presence of iron in these materials does not lead to change the shape of the particles at any loading.

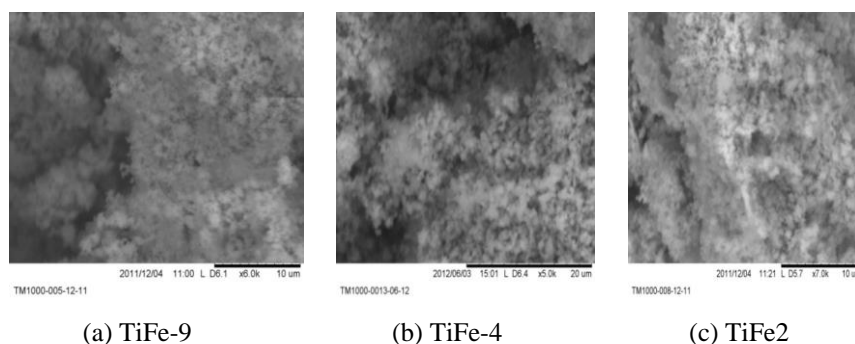


Figure 7. SEM micrographs

### 2.1. Catalytic activity

The catalytic activity of the different catalysts was studied in the cyclohexene oxidation by molecular oxygen. This reaction can lead to the formation of different products (Scheme 1). These products are obtained via an epoxidation reaction or an allylic oxidation reaction.

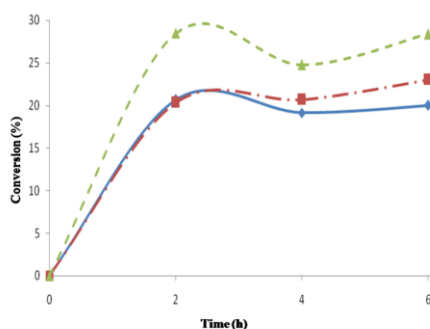


Figure 8. Conversion of cyclohexene using (---■---)TiFe<sub>2</sub>, (.\_.■.\_.)TiFe<sub>4</sub>, (—◆—)TiFe<sub>9</sub>

First, we noticed that  $\text{TiO}_2$  has no activity and the TiFe materials can catalyze the oxidation of cyclohexene by molecular oxygen. Moreover, cyclohexene conversion reached the maximum after 2 hours of reaction and no longer changes (Table 6). These results are obtained whatever the iron content introduced with  $\text{TiO}_2$ . We note also that the catalyst containing the highest amount of iron  $\text{TiFe}_2$  is the most active one (Figure. 8).

Table 5. Cyclohexene oxidation during the first hours of the catalyst contact

t(h)	Conversion (%)				TOF( $\text{h}^{-1}$ )		
	Ti	TiFe <sup>9</sup>	TiFe <sup>4</sup>	TiFe <sup>2</sup>	TiFe <sup>9</sup>	TiFe <sup>4</sup>	TiFe <sup>2</sup>
0	0	0	0	0	0	0	0
2	0	21	20	28.5	1.29	1.35	2.01
4	0	19	21	25	1.19	1.37	1.75
6	0	20	24	28	1.27	1.57	2.01
24	0	22.3	23	32.5	1.39	1.51	2.30

Furthermore, the reaction was continued until 24 hours, at this time the quantities of the different products are measured and the selectivities are calculated. We observed (Table 5) that more than 90% of adipic acid is produced and about 10% of the products are issued from a premiere oxidation of cyclohexene (cyclohexenone and cyclohexenol).

Table 6. The product distribution of the cyclohexene oxidation after 24 h of reaction

Materials	Conv %	TOF( $\text{h}^{-1}$ )	A.A[a]%	Enone[b] %	Enol[c] %
TiFe <sup>9</sup>	22.3	1.39	89.3	7.7	3.0
TiFe <sup>4</sup>	23	1.51	91.8	5.3	2.9
TiFe <sup>2</sup>	32.5	2.30	91.4	6.2	2.4

[a] Adipic Acid. [b] Cyclohexenone. [c] Cyclohexenol.

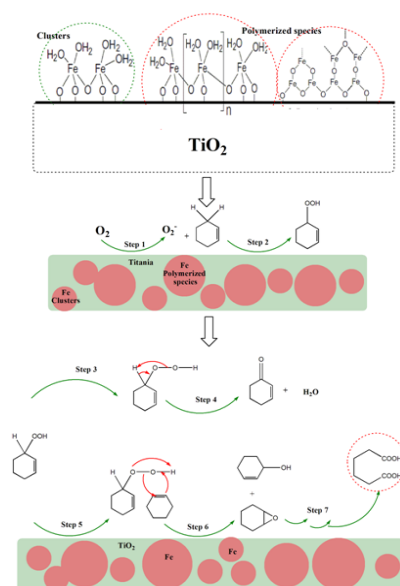
In comparison with the same materials, but prepared by different ways (sol gel), we observe that all doped materials show an improvement of the activity in the presence of iron species and that the preparation of this kind of materials by sol gel way lead to achieve more activity than those prepared par impregnations; especially in the case of  $\text{TiFe}_2$  (conversion about 42%). Furthermore, Ti prepared by sol gel lead to an important activity than Ti (P25, commercial); which can be related to the important area of titania prepared by sol gel way ( $148 \text{ m}^2/\text{g}$ ).

Scheme 2 presents the principal intermediates that can lead to the formation of adipic acid. Hence, we noticed that at present we don't find a final mechanism how

can explain the formation of the products. So, as we were explained in our previous work the first step of cyclohexene oxidation lead to form cyclohexane epoxyde that after hydrolysis step produce cyclohexene diol. The oxidation of diol lead after several intermediates to achieved adipic acid. In the same scheme, we showed the nature of the iron species on the catalyst surface that can be clusters and polymerized species (proved by UV-Vis characterization) supported on titania; we suppose that those iron particles are responsible to the improvement of the catalytic activity.

We proposed a reaction pathway based on several works in the literature. In scheme 2 we proposed reaction pathway for the catalytic oxidation of cyclohexene with molecular oxygen in the presence of TiO<sub>2</sub>-Fe<sub>2</sub>O<sub>3</sub> catalysts. As it was demonstrated by characterization method, on the titania surface, we obtained two kinds of iron species: clusters and polymerized species. We conclude that those species are the main key to the enhancement of the P25 catalytic activity.

In the first step, as it was evocated in several research paper (Sato *et al.*, 1998; Noyori *et al.*, 2003; Prieto-Centurion *et al.*, 2012; Ameer *et al.*, 2013, Van de Vyver and Román-Leshkov, 2013; Ameer *et al.*, 2014), an oxygen activation at the composite surface produced radical form which migrates into solution. The next step is the insertion of activated oxygen into the allylic bond "C-H" of cyclohexene to give the adsorbed hydroperoxide. Hence, this intermediate can have a rearrangement to the ketone and water (step 4) or reacted with another cyclohexene molecule to give unsaturated alcohol and cyclohexane epoxyde. To obtain the final product of oxidation, adipic acid, it was proposed that a series of oxidation and hydrolysis reactions occurs of cyclohexane epoxyde.



Scheme 2. Cyclohexene oxidation by molecular oxygen on TiO<sub>2</sub>-Fe<sub>2</sub>O<sub>3</sub> catalysts

## 2.2. Conclusion

$\text{Fe}_2\text{O}_3/\text{TiO}_2$  materials were prepared by an impregnation of  $(\text{Fe}(\text{NO}_3)_3 \cdot 9\text{H}_2\text{O})$  on  $\text{TiO}_2$ . Different materials with different amount of  $\text{Fe}_2\text{O}_3$  were prepared. The characterizations of these materials by DR/UV-Vis, DRX, FT-IR showed that iron is introduced in the  $\text{TiO}_2$  lattice. Otherwise the BET showed that iron makes a little change in the  $\text{TiO}_2$  area. These materials showed a great activity in the oxidation of cyclohexene by molecular oxygen toward adipic acid under a mild and a green condition.

## 3. Experimental Section

### 3.1. Preparation of $x\%\text{Fe}_2\text{O}_3/\text{TiO}_2$ materials

The  $x\%\text{Fe}_2\text{O}_3/\text{TiO}_2$  oxides are prepared by impregnation method. First, 2 g of  $\text{TiO}_2$  (P25, Degussa) are mixed with 25 mL of distilled water (solution a). A solution (b) is prepared by dissolving a required amount of iron nitrate ( $\text{Fe}(\text{NO}_3)_3 \cdot 9\text{H}_2\text{O}$ ) in 10 mL of distilled water. Afterwards, the solution (b) is added to the solution (a) dropwise under stirring. The mixture is aged for 2 h at room temperature, dried at  $100^\circ\text{C}$  overnight and finally calcined at  $400^\circ\text{C}$  ( $10^\circ\text{C}/\text{min}$ ) for 4 h.

### 3.2. Catalysts characterizations

The chemical compositions of the samples were determined by inductively coupled plasma emission spectroscopy (ICP) using a Varian ICP-AES. The samples were characterized by XRD. Patterns of the calcined samples were recorded on a Bruker AXS D5005 diffractometer. The BET areas were determined from  $\text{N}_2$  adsorption isotherms at 77 K using a Quantachrom NOVA 1000 instrument. The diffuse reflectance UV-visible spectra (200–800 nm) were collected on a Perkin Elmer spectrometer. The FTIR spectra of the solids were recorded using an Agilent Technologies Cary 60 series FTIR spectrometer with ATR accessories.

### 3.3. Oxidation of cyclohexene by $\text{O}_2$

As was described in our previous work; the oxidation of cyclohexene reactions was carried out in a Parr 5500 series compact vessel (Capacity=0.14 L, pressure maximum 200 bar). In a typical oxidation reaction, 4.5 mL cyclohexene, 73 mL n-heptane and 0.1 g catalyst were charged into the reactor. The reactor was closed, purged three times and then heated up to  $80^\circ\text{C}$ . Afterwards, the reactor was pressurized with oxygen ( $P = 0.6 \text{ MPa}$ ) and the stirring was started (Figure. 9). Samples were taken every 2 hours then analyzed by gas chromatography (GC) using a SCHIMADZU 14-B gas chromatograph equipped with HP-FFAP capillary column.

After the completion of the reaction 24 h the products were collected and analyzed by GCMS. Mass spectra were recorded on a QTOF Micro (Waters).

More over an iodometric titration was done with every collected sample in order to verify the formation of hydroperoxide species in the reaction medium. In all cases we remarked that there is no hydroperoxide species.

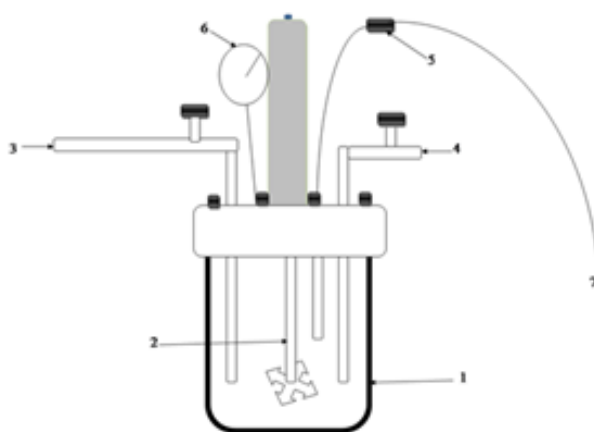


Figure 9. Oxidation apparatus: 1, pressure reactor (oxygen reservoir 1); 2, agitation; 3, oxygen reservoir; 4, simple taker; 5, temperature control; 6, pressure control; 7, thermocouple (Ameur 2014)

## Reference

- Ahmed M., El-Katori E. E., Gharni Z. H. (2013). Photocatalytic degradation of methylene blue dye using Fe<sub>2</sub>O<sub>3</sub>/TiO<sub>2</sub> nanoparticles prepared by sol-gel method. *Journal of Alloys and Compounds*, Vol. 553, pp. 19-29. <http://dx.doi.org/10.1016/j.jallcom.2012.10.038>
- Ameur N. (2014). Thèse de Doctorat, Préparation de nano matériaux a base d'or et de fer application en réactions d'oxydation allylique d'olefines. *Université de Tlemcen, Algérie*.
- Ameur N., Bedrane S., Bachir R., Choukhou-Braham A. (2013). Influence of nanoparticles oxidation state in gold based catalysts on the product selectivity in liquid phase oxidation of cyclohexene. *Journal of Molecular Catalysis*, Vol. 374, pp. 1-6. <https://doi.org/10.1016/j.molcata.2013.03.008>
- Ameur N., Berrichi A., Bedrane S., Bachir R. (2014). Preparation and characterization of Au/Al<sub>2</sub>O<sub>3</sub> and Au-Fe/Al<sub>2</sub>O<sub>3</sub> materials, active and selective catalysts in oxidation of cyclohexene. *Advanced Materials Research*, Vol. 856, pp. 48-52. <https://doi.org/10.4028/www.scientific.net/AMR.856.48>

- Bart J. C., Cavallaro S. (2015). Transiting from adipic acid to bioadipic acid. part II. biosynthetic pathways. *Industrial & Engineering Chemistry Research*, Vol. 54, pp. 567-576. <https://doi.org/10.1021/ie502074d>
- Behera G. C., Parida K., Satapathy P. K. (2013). Sustainable and efficient protocol for the synthesis of a RGO–VPO composite with synergetic stability and reactivity. *RSC Advances*, Vol. 3, pp. 4863-4866. <https://doi.org/10.1039/c3ra00092c>
- Bohström Z., Rico-Lattes I., Holmberg K. (2010). Oxidation of cyclohexene into adipic acid in aqueous dispersions of mesoporous oxides with built-in catalytical sites. *Green Chemistry*, Vol. 12, pp. 1861-1869. <https://doi.org/10.1039/c0gc00032a>
- Cai Z. Y., Zhu M. Q., Chen J., Shen Y. Y., Zhao J., Tang Y., Chen X. Z. (2011). Solvent-free oxidation of cyclohexene over catalysts Au/OMS-2 and Au/La-OMS-2 with molecular oxygen. *Catalysis Communications*, Vol. 12, pp. 197-201. <https://doi.org/10.1016/j.catcom.2010.09.014>
- Castellan A., Bart J. C. J., Cavallaro S. (1991). Industrial production and use of adipic acid. *Catalysis Today*, Vol. 9, pp. 237-254. [https://doi.org/10.1016/0920-5861\(91\)80049-F](https://doi.org/10.1016/0920-5861(91)80049-F)
- Cheng C. Y., Lin K. J., Prasad M. R., Fu S. J., Chang S. Y., Shyu S. G., Sheu H. S., Chen C. H., Chuang C. H., Lin M. T. (2007). Synthesis of a reusable oxotungsten-containing SBA-15 mesoporous catalyst for the organic solvent-free conversion of cyclohexene to adipic acid. *Catalysis Communications*, Vol. 8, pp. 1060-1064. <https://doi.org/10.1016/j.catcom.2006.10.027>
- Cozzolino M., Di Serio M., Tesser R., Santacesaria E. (2007). Grafting of titanium alkoxides on high-surface SiO<sub>2</sub> support: An advanced technique for the preparation of nanostructured TiO<sub>2</sub>/SiO<sub>2</sub> catalysts. *Applied Catalysis A: General*, Vol. 325, pp. 256-262. <https://doi.org/10.1016/j.apcata.2007.02.032>
- Dapurkar S. E., Kawanami H., Komura K., Yokoyama T., Ikushima Y. (2008). Solvent-free allylic oxidation of cycloolefins over mesoporous CrMCM-41 molecular sieve catalyst at 1 atm dioxygen. *Applied Catalysis A: General*, Vol. 346, No. 1, pp. 112-116.
- Ghosh S., Acharyya S. S., Adak S., Konathala L. S., Sasaki T., Bal R. (2014). Selective oxidation of cyclohexene to adipic acid over silver supported tungsten oxide nanostructured catalysts. *Green Chemistry*, Vol. 16, pp. 2826-2834. <https://doi.org/10.1039/C4GC00130C>
- Jähnisch K., Hessel V., Löwe H., Baerns M. (2004). Chemistry in microstructured reactors. *Angewandte Chemie International Edition*, Vol. 43, pp. 406-446.
- Jiang D., Mallat T., Meier D. M., Urakawa A., Baiker A. (2010). Copper metal–organic framework: Structure and activity in the allylic oxidation of cyclohexene with molecular oxygen. *Journal of Catalysis*, Vol. 270, No. 1, pp. 26-33.
- Jin P., Zhao Z. H., Dai Z. P., Wei D., Tang M., Wang X. (2011). Influence of reaction conditions on product distribution in the green oxidation of cyclohexene to adipic acid with hydrogen peroxide. *Catalysis Today*, Vol. 175, pp. 619-624. <https://doi.org/10.1016/j.cattod.2011.04.041>
- Lapisardi G., Chiker F., Launay F., Nogier J., Bonardet J. (2005). Preparation, characterisation and catalytic activity of new bifunctional Ti-*Al*SBA15 materials. Application to a "one-pot" green synthesis of adipic acid from cyclohexene and organic hydroperoxides. *Microporous and Mesoporous Materials*, Vol. 78, pp. 289-295. <https://doi.org/10.1016/j.micromeso.2004.10.012>

- Li B., He P., Yi G., Lin H., Yuan Y. (2009). Performance of gold nanoparticles supported on carbon nanotubes for selective oxidation of cyclooctene with use of O<sub>2</sub> and TBHP. *Catalysis Letters*, Vol. 133, pp. 33. <https://doi.org/10.1007/s10562-009-0171-0>
- Meng L., Zhai S., Sun Z., Zhang F., Xiao Z. An Q. (2015). Green and efficient synthesis of adipic acid from cyclohexene over recyclable H3PW4O24/PEHA/ZrSBA-15 with platelet morphology. *Microporous and Mesoporous Materials*, Vol. 204, pp. 123-130. <https://doi.org/10.1016/j.micromeso.2014.11.010>
- Noyori R., Aoki M., Sato K. (2003). Green oxidation with aqueous hydrogen peroxide. *Chemical Communications*, Vol. 34, No. 16, pp. 1977-1986.
- Nur H. (2006). Modification of titanium surface species of titania by attachment of silica nanoparticles. *Materials Science and Engineering: B*, Vol. 133, No. 1-3, pp. 49-54.
- Prieto-Centurion D., Boston A. M., Notestein J. M. (2012). Structural and electronic promotion with alkali cations of silica-supported Fe (III) sites for alkane oxidation. *Journal of Catalysis*, Vol. 296, pp. 77-85.
- Reed S. M., Hutchison J. E. (2000). Green chemistry in the organic teaching laboratory: An environmentally benign synthesis of adipic acid. *Journal of Chemical Education*, Vol. 77, pp. 1627. <https://doi.org/10.1021/ed077p1627>
- Sato K., Aoki M., Noyori R. (1998). A "Green" route to adipic acid: direct oxidation of cyclohexenes with 30 percent hydrogen peroxide. *Science*, Vol. 281, pp. 1646-1647. <https://doi.org/10.1126/science.281.5383.1646>
- Schwidder M., Kumar M. S., Klementiev K., Pohl M. M., Brückner A., Grünert W. (2005). Selective reduction of NO with Fe-ZSM-5 catalysts of low Fe content: I. Relations between active site structure and catalytic performance. *Journal of Catalysis*, Vol. 231, pp. 314-330.
- Sreethawong T., Yamada Y., Kobayashi T., Yoshikawa S. (2006). Optimization of reaction conditions for cyclohexene epoxidation with H<sub>2</sub>O<sub>2</sub> over nanocrystalline mesoporous TiO<sub>2</sub> loaded with RuO<sub>2</sub>. *Journal of Molecular Catalysis A: Chemical*, Vol. 248, pp. 226-232.
- Vafaezadeh M., Hashemi M. M. (2014). Simple and green oxidation of cyclohexene to adipic acid with an efficient and durable silica-functionalized ammonium tungstate catalyst. *Catalysis Communications*, Vol. 43, pp. 169-172. <https://doi.org/10.1016/j.catcom.2013.10.001>
- Vafaezadeh M., Hashemi M. M., Shakourian-Fard M. (2012). Mesoporous silica-functionalized dual Brønsted acidic ionic liquid as an efficient catalyst for thioacetalization of carbonyl compounds in water. *Catalysis Communications*, Vol. 26, pp. 54-57. <https://doi.org/10.1016/j.catcom.2013.07.004>
- Van de Vyver S., Román-Leshkov Y. (2013). Emerging catalytic processes for the production of adipic acid. *Catalysis Science & Technology*, Vol. 3, pp. 1465-1479. <https://doi.org/10.1039/C3CY20728E>
- Wang Q., Gürsel I. V., Shang M., Hessel V. (2013). Life cycle assessment for the direct synthesis of adipic acid in microreactors and benchmarking to the commercial process. *Chemical Engineering Journal*, Vol. 234, pp. 300-311.
- Weiner H., Trovarelli A., Finke R. G. (2003). Expanded product, plus kinetic and mechanistic, studies of polyoxoanion-based cyclohexene oxidation catalysis: The detection of ~70 products at higher conversion leading to a simple, product-based test for the presence of

olefin autoxidation. *Journal of Molecular Catalysis A: Chemical*, Vol. 191, No. 2, pp. 217-252. [https://doi.org/10.1016/S1381-1169\(02\)00344-8](https://doi.org/10.1016/S1381-1169(02)00344-8)

Wen Y., Wang X., Wei H., Li, B., Jin P., Li L. (2012). A large-scale continuous-flow process for the production of adipic acid via catalytic oxidation of cyclohexene with H<sub>2</sub>O<sub>2</sub>. *Green Chemistry*, Vol. 14, pp. 2868-2875. <https://doi.org/10.1039/c2gc35677e>